Geophysical Research Letters

RESEARCH LETTER
10.1029/2022GL098908

Mooring Measurements of Anadyr Current Nitrate, Phosphate, and Silicate Enable Updated Bering Strait Nutrient Flux Estimates

Tyler D. Hennon[1], Seth L. Danielson[1], Rebecca A. Woodgate[2], Brita Irving[1], Dean A. Stockwell[1], and Calvin W. Mordy[3,4]

[1]College of Fisheries and Ocean Sciences, University of Alaska Fairbanks (UAF), Fairbanks, AK, USA, [2]Applied Physics Laboratory (APL), University of Washington (UW), Seattle, WA, USA, [3]Cooperative Institute for Climate, Ocean, & Ecosystem Studies, University of Washington (UW), Seattle, WA, USA, [4]Pacific Marine Environmental Laboratory (PMEL), National Oceanographic and Atmospheric Administration (NOAA), Seattle, WA, USA

Abstract In situ nutrient concentration data and salinity-nutrient parameterizations established at Anadyr Strait from June 2017 to June 2018 are used to estimate monthly Pacific-to-Arctic fluxes of nitrate, phosphate, and silicate through Bering Strait over 1997–2019. In most months our estimates rely on measurements made from mooring-based sensors and whole water samples, while over May–August the basis is shipboard hydrography. We find annually averaged Bering Strait fluxes of 16 ± 6, 1.5 ± 0.5, and 30 ± 11 kmol/s for nitrate, phosphate, and silicate, respectively, with inter-annual variability ±30% of the mean. Maximum fluxes occur in April, exceeding the annual average by ∼50%, while minimum fluxes occur in December. Annually averaged fluxes estimated here are ∼50% higher than previous estimates. Significant ($p < 0.05$) increasing trends in phosphate and silicate fluxes are found over 1998–2018, but not nitrate. However, it is unclear if these trend results are due to differences in draw-down or limitations of the salinity-nutrient parameterizations.

Plain Language Summary Nutrients flowing through Bering Strait (Pacific to Arctic) regulate the growth of Arctic plankton, which form the base of the marine food web. However, because of limited nutrient data at Bering Strait, only a few studies have attempted to estimate the size of this nutrient supply. We find that nutrients and salinity are closely related at nearby Anadyr Strait. Using those relationships and long-term mooring observations of salinity and currents at Bering Strait, we are able to estimate Bering Strait nutrient concentrations and the amount carried through the strait into the Arctic. We find strong seasonal cycles as well as significant year-to-year variability. Our estimates are about 50% higher than past studies, suggesting more Pacific-Arctic nutrient delivery than previously thought.

Key Points:

- We use in situ and salinity-based estimates of nutrient concentrations to estimate nutrient fluxes through Bering Strait
- We estimate annually averaged fluxes of 16 ± 6 (nitrate), 1.5 ± 0.5 (phosphate), and 30 ± 11 kmol/s (silicate), ∼50% larger than prior studies
- Bering Strait nutrient flux varies by season, with largest poleward fluxes occurring in April, and weakest fluxes occurring in December

Supporting Information:

Supporting Information may be found in the online version of this article.

Correspondence to:

T. D. Hennon,
tdhennon@alaska.edu

Citation:

Hennon, T. D., Danielson, S. L., Woodgate, R. A., Irving, B., Stockwell, D. A., & Mordy, C. W. (2022). Mooring measurements of Anadyr current nitrate, phosphate, and silicate enable updated Bering Strait nutrient flux estimates. *Geophysical Research Letters*, *49*, e2022GL098908. https://doi.org/10.1029/2022GL098908

Received 29 MAR 2022
Accepted 16 JUN 2022

Author Contributions:

Data curation: Seth L. Danielson, Brita Irving, Calvin W. Mordy
Formal analysis: Tyler D. Hennon, Seth L. Danielson
Visualization: Tyler D. Hennon
Writing – original draft: Tyler D. Hennon, Seth L. Danielson
Writing – review & editing: Tyler D. Hennon, Seth L. Danielson, Rebecca A. Woodgate, Brita Irving, Dean A. Stockwell, Calvin W. Mordy

© 2022. American Geophysical Union. All Rights Reserved.

1. Introduction

The Arctic is experiencing rapid change (Polyakov et al., 2020), including reduced sea ice extent and volume (Wang et al., 2018), and altered growing conditions for marine phytoplankton (Lewis & Arrigo, 2020), affecting Arctic marine ecosystems (Huntington et al., 2020), including iconic marine mammals and seabirds, subsistence harvests vital to Indigenous communities, and biological carbon pump dynamics.

Bering Strait is the only oceanic link between the Arctic and Pacific oceans, and is relatively narrow (∼85 km across) and shallow (∼50 m deep) with an annual average throughflow around 1.0 Sv (10^6 m^3/s) (Woodgate, 2018). The Anadyr Current (Figure 1a) delivers approximately 80% of the Bering Strait transport through Anadyr Strait ∼250 km south of the Bering Strait (Danielson et al., 2014). The advective time between them is ≥10 days (Coachman, 1993). Due to typically low nutrient concentrations on the eastern Bering shelf (Danielson et al., 2011), the Anadyr Current delivers the bulk of nutrients that are advected into the Arctic through Bering Strait, supporting remarkably high levels of pelagic and benthic biological productivity in the Pacific Arctic (Grebmeier et al., 2015).

Little prior work has evaluated Arctic-bound nutrient fluxes directly at Bering Strait. Torres-Valdes et al. (2013) used a single August 2005 cross-strait transect in combination with modeled currents to estimate annually averaged fluxes into the Chukchi Sea: 9.0 ± 0.8, 1.3 ± 0.1, and 20.9 ± 2.4 kmol/s for nitrate, phosphate, and silicate, respectively. Using a three-dimensional ocean-sea ice-biogeochemical model, Zhou et al. (2021) estimated an

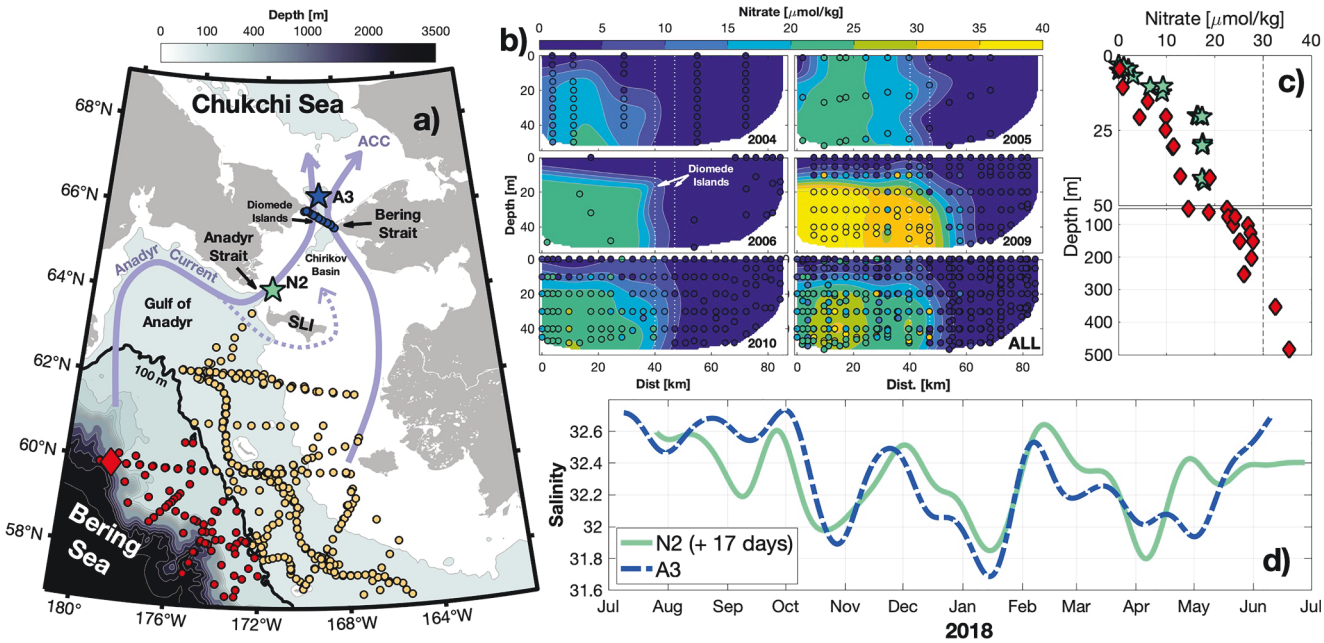

Figure 1. (a) Map of hydrography, typical flow patterns and mooring locations. Yellow/red circles are sites of hydrographic profiles collected mostly during summer from 2008 to 2018 (sources in Table T1 of Supporting Information S1; red markers denote casts to >100 m); blue circles mark Bering Strait Russian-American Long-Term Census of the Arctic Program (RUSALCA) stations. Stars mark mooring sites N2 (cyan) and A3 (blue). Thick black contour is at 100 m depth. Light blue lines show nominal paths of major currents. Abbreviations: SLI = Saint Laurence Island, ACC = Alaskan Coastal Current. (b) August RUSALCA Bering Strait observations from 2004 to 2010. Dots mark nutrient samples, and contours are objective maps calculated from observations. Lower right subpanel aggregates all years. (c) Nitrate profiles collected at N2 (cyan stars, June 2017) and Bering continental slope (red diamonds, collected June, 2010). Location of continental slope observations is denoted by the large red diamond in (a). (d) Lowpass filtered (30 day cutoff period) salinity at N2 (cyan, lagged by 17 days) and A3 (blue dashed).

annual flux of ∼10 kmol/s of nitrate. Downstream in the Chukchi Sea, Mordy et al. (2020) found inter-annual variability in winter nitrate flux of up to 10 kmol/s during 2010–2018. Here, we provide observation-based nutrient flux estimates from a year of mooring-based measurements from Anadyr Strait (2017–2018) and long term (1997–2019) mooring observations in Bering Strait.

2. Data

2.1. Shipboard Hydrography

Nutrient and conductivity-temperature-depth (CTD) hydrographic data (>500 vertical profiles) from ship-based observation programs (April–September) in the Northern Bering and Southern Chukchi seas between 2004 and 2018 are used to characterize regional nutrient distributions (Figure 1a, Table T1 in Supporting Information S1).

2.2. Moorings

2.2.1. Anadyr Strait Mooring

Subsurface mooring N2 was deployed in 46 m of water in Anadyr Strait (Figure 1a) from 12 June 2017–9 June 2018 at 64.1545°N, 174.5260°W. N2 was equipped with Sea-Bird Electronics (SBE) CTD dataloggers, a Teledyne RDI acoustic Doppler current profiler (ADCP), a Satlantic submersible ultraviolet nitrate analyzer (SUNA), and a Green Eyes Aqua Monitor discrete water sampler (Table T2 in Supporting Information S1).

Instrumentation specifics were as follows: CTDs at depths of 25 m (SBE-16, 120 min sampling), 35 and 41 m (SBE-37, 15 min sampling); an upward-looking 300 kHz ADCP at 41 m depth (30 min ensembles of 1 m bins); a SUNA V2 at 35 m depth (120 min sampling); and an Aqua Monitor at 35 m depth, which over the deployment collected 25 500 mL water samples in rack-mounted IV bags, each primed with 400 μL of saturated mercuric chloride solution to halt microbial activity. Following mooring recovery, 60 mL subsamples were filtered (0.45 mm cellulose acetate filters) and stored frozen. On shore, thawed samples were analyzed for nitrate (NO_3^-),

nitrite (NO_2^-), ammonium (NH_4^+), phosphate (PO_4^{3-}), and silicate (H_4SiO_4) using automated continuous flow analysis (Becker et al., 2020). Quality controls are described in the archived datasets. Between 30 and 90 min after deployment, the Aqua Monitor collected four samples to estimate repeatability. Thereafter, sample spacing was between 9 and 31 days (more frequently in summer).

2.2.2. Bering Strait Mooring

We use monthly estimates of Bering Strait salinity and transport (Woodgate, 2018; Woodgate et al., 2015) from the long-term (1997 to present) A3 mooring (Figure 1a), which is representative of average Bering Strait through-flow properties (Woodgate et al., 2015). These estimates do not include contributions from the Alaskan Coastal Current (ACC), which is responsible for ∼10% of the net transport but is nitrate-deplete (Danielson et al., 2017).

3. Results

3.1. Nutrient Biases and Corrections

Niskin bottle nutrient samples from the N2 mooring deployment and recovery cruises are used to correct the SUNA and Aqua Monitor data for offsets and drift (e.g., Daniel et al., 2020). CTD profile and Niskin samples (not shown) exhibit a well-mixed water column within ±10 m of the Aqua Monitor at deployment, with average $NO3_{NIS}$ = 17.3 ± 0.4, $PO4_{NIS}$ = 1.76 ± 0.02, and $SiO4_{NIS}$ = 27.4 ± 0.6 µmol/kg from six samples (± indicates 95% confidence interval hereinafter). The first four Aqua Monitor samples (from just after deployment) had concentrations of $NO3_{AM}$ = 14.5 ± 1.8, $PO4_{AM}$ = 1.94 ± 0.11, and $SiO4_{AM}$ = 23.6 ± 2.2 µmol/kg. These samples suggest initial Aqua Monitor biases of about −2.8, +0.18, and −3.8 µmol/kg, and measurement uncertainties of 1.8, 0.1, and 2.2 (nitrate, phosphate, and silicate, respectively). Upon recovery 1 year later, CTD profiles suggest a well-mixed water column within ±5 m of the Aqua Monitor, with average $NO3_{NIS}$ = 12.9 ± 0.2, $PO4_{NIS}$ = 1.75 ± 0.04, and $SiO4_{NIS}$ = 26.8 ± 0.8 µmol/kg from five samples, where a single Aqua Monitor sample measured $NO3_{AM}$ = 13.1, $PO4_{AM}$ = 1.92, $SiO4_{AM}$ = 23.6 µmol/kg. Aqua Monitor nutrient concentrations were adjusted assuming linear drift between deployment and recovery during the yearlong occupation. The SUNA nitrate estimate bias was 4.0 on deployment and 0.3 µmol/kg on recovery, and concentrations were again adjusted assuming linear drift. Post-correction, the two measures of nitrate at mooring N2 (Aqua Monitor and SUNA) are strongly correlated over the year-long deployment (root-mean-square-difference = 2.3 µmol/kg, $r = 0.87$ and $p < 0.01$, Figure 2e).

3.2. Salinity-Nutrient Relations

Ship-based hydrography from across the northern Bering Sea shelf and continental slope exhibit a nearly linear relationship between salinity (S_{HYD}) and nitrate ($NO3_{HYD}$) for measurements collected from >100 m depth (Figure 2a, dark grey dots), where S_{HYD} = 33–34 practical salinity units (PSU) and $NO3_{HYD}$ = 25–45 µmol/kg. Extrapolation of this mixing line to full nitrate depletion at salinity ∼31 PSU closely approximates the maximum observed nitrate concentration at each salinity in the range of 31–34 PSU (Figure 2a), suggesting that in the absence of biological nitrate drawdown, mixing between nitrate-rich slope waters and nitrate-deplete shelf waters (upper 10–20 m across the eastern Bering shelf) primarily regulates nutrient concentration. While the range of depths that the Anadyr Current draws its source waters from is not well known, near-bottom observations of nitrate up to 30 µmol/kg in Anadyr Strait (Walsh et al., 1989) and typical vertical profiles from the slope region (Figure 1c) suggest that the core of the Anadyr Current must draw slope waters from ≥100 m depth. This assumes no mixing between the region of upwelling and Anadyr Strait, so if Anadyr Current waters mix with lower-salinity shelf waters during their transit to Anadyr Strait, the mean source depth could be greater.

At N2, there is no significant relationship between nutrient (Aqua Monitor) and salinity (SBE37) in situ measurements at 35 m depth (i.e., sub-pycnocline) when considering all samples together. However, significant relationships emerge when data are partitioned seasonally (Figures 2b–2d). We divide mooring data into three intervals that roughly map onto fall, winter and summer, respectively: September–December (cooling, ice-free, decreasing light availability; magenta circles) and January–April (cold, ice-covered; orange triangles); May–August (warming, ice-free or declining sea ice conditions, high light availability; green squares).

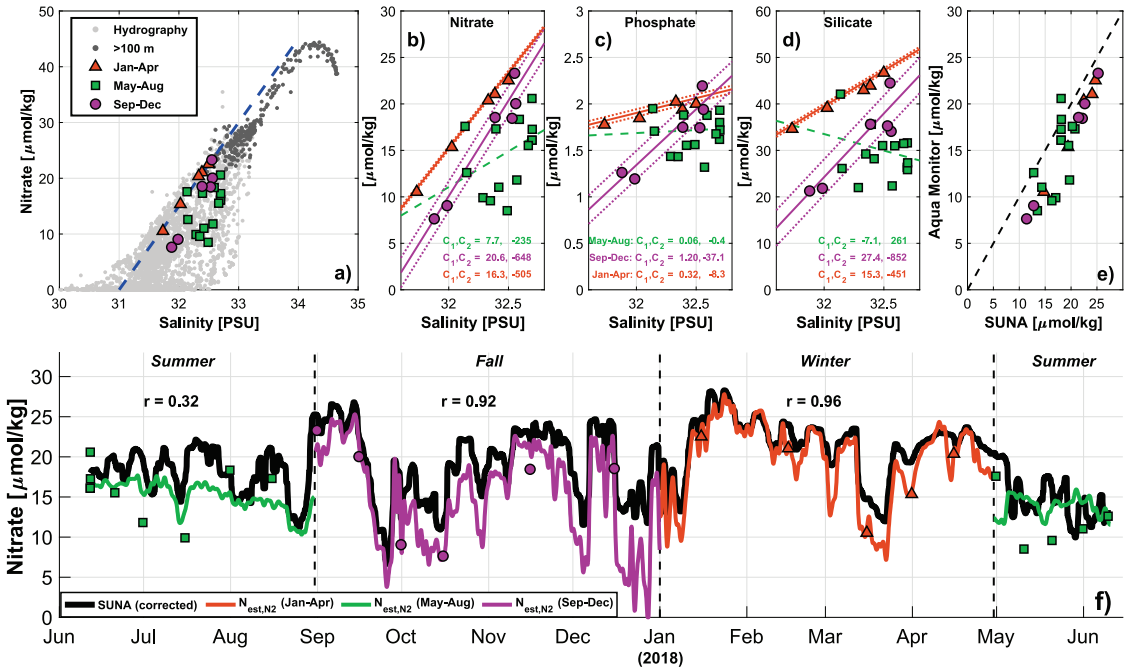

Figure 2. (a) Hydrographic samples of nitrate and salinity from across the Bering Sea in gray (see Figure 1a). Darker markers indicate samples from ≥100 m depth. Colored markers show 25 nitrate/salinity pairs taken by the moored Aqua Monitor and SBE at N2. Squares, circles and triangles correspond to May–August, September–December and January–April, respectively. The dashed line shows rough mixing line between slope and inner shelf waters. (b) $NO3_{AM}$ versus S_{N2} (c) $PO4_{AM}$ versus S_{N2} (d) $SiO4_{AM}$ versus S_{N2}. In (b–d), solid lines are significant ($p < 0.05$) best-fits for each season, dotted lines are 95% confidence intervals, and dashed lines are fits where $p > 0.05$. Constants from Equation 1, C_1 ([μmol/kg]/[PSU]) and C_2 are denoted for each season. (e) $NO3_{AM}$ versus $NO3_{SUNA}$ (dashed line is 1:1). (f) Observed nitrate ($NO3_{SUNA}$, thick black line) and estimated nitrate ($NO3_{EST,N2}$, colored lines); *r*-values show correlations between the two seasonally. Vertical dashed lines mark seasonal delineations.

The moored S_{N2} data are strongly correlated with $NO3_{AM}$ from September–December ($r = 0.97$, $p < 0.01$, $N = 5$) and January–April ($r = 0.99$, $p < 0.01$, $N = 6$), but are not well correlated for May–August ($r = 0.50$, $p = 0.10$, $N = 13$). We attribute the difference between fall and winter regression lines to the fall season being at the end of the growing season after the nutrient inventory has experienced summer biological drawdown. The strong correlations show that for fall and winter (both weakly stratified), salinity provides a useful proxy for nitrate in the Anadyr Current.

Using SBE salinity (S_{N2}) and calibrated Aqua Monitor nitrate (Section 3.1) at mooring N2, we perform linear least squares regressions to parameterize nitrate concentration ($NO3_{EST,N2}$), that is,

$$NO3_{EST,N2} = C_1 S_{N2} + C_2 \quad (1)$$

C_1 and C_2 are coefficients calculated for each of the three seasonal intervals (Figures 2b–2d).

We find $NO3_{EST,N2}$ closely tracks both synoptic-scale and longer period signals captured by the SUNA nitrate sensor ($NO3_{SUNA,N2}$) during fall and winter intervals (Figure 2f). Differences between $NO3_{SUNA,N2}$ and $NO3_{EST,N2}$ are not uniform from September–May (up to 10 μmol/kg in December). It is unclear why there is a consistent bias between $NO3_{SUNA,N2}$ and $NO3_{EST,N2}$ (average 2.5 μmol/kg). Though it may point to limitations of our CTD calibrations, we note it is on the same scale as the Aqua Monitor precision (Section 3.1). The large deviation in December may be related to seasonally voluminous Alaskan river discharges in the eastern Bering Sea that subsequently advect westward (Danielson et al., 2006) carrying a different nitrate-salinity relation than found in the Anadyr Current.

As with nitrate, correlations with S_{N2} are significant ($p < 0.05$) for $PO4_{AM}$ and $SiO4_{AM}$ for both September–December ($PO4_{AM}$:0.92; $SiO4_{AM}$:0.91) and January–April ($PO4_{AM}$:0.92; $SiO4_{AM}$:0.99), but neither are significantly correlated during May–August. Salinity-based estimates of phosphate ($PO4_{EST,N2}$) and silicate ($SiO4_{EST,N2}$) are calculated in identical fashion to $NO3_{EST,N2}$ (Equation 1).

3.3. Nutrient Fluxes Through Anadyr Strait

Using velocity data from the N2 ADCP and the salinity-nutrient regressions (Section 3.2), we can estimate nutrient fluxes through Anadyr Strait. Anadyr Strait is 73 km wide, has a median depth of 40 m, and is approximately 2.7×10^6 m^2 in cross-sectional area. The major axis of sub-tidal barotropic currents (from the ADCP on N2) is roughly normal to Anadyr Strait (oriented with through-flow). We take currents along this axis as representative for the whole Anadyr Strait, and thus estimate volume transport through the strait (T_{AS}). Our approach assumes the current is homogeneous across the strait, which seems a reasonable first-order approximation given the prominent forcings of flow through Anadyr Strait are large-scale (i.e., basin-scale pressure gradients). The average current speed along the major axis is 39 cm/s for the year-long deployment, translating to 1.1 Sv of volume transport. This is similar to the A3-based Bering Strait transport estimate for this timespan (1.3 ± 0.3 Sv).

To estimate nutrient flux through Anadyr Strait, we combine the monthly salinity-based estimates of nutrient concentration at N2 (Section 3.2) with the monthly mean volume transport, T_{AS}. Nitrate flux ($F_{NO3,AS}$), for example, is defined as:

$$F_{NO3,AS} = \rho_0 \, T_{AS} \, NO3_{est,N2} \tag{2}$$

where ρ_0 is the nominal density of Bering shelf water (1025 kg/m^3). Based on N2 ADCP measurements, we further assume an unstratified water column from November–April such that salinity and nitrate measurements at 35 m depth are representative of the full water column. For May–October, we assume the water column is stratified and the upper 10 m of the water column is fully nitrate-deplete. Phosphate ($F_{PO4,AS}$) and silicate ($F_{SiO4,AS}$) fluxes are calculated similarly.

From September, 2017 to April 2018 (when salinity-nutrient regressions are significant), average nitrate, phosphate, and silicate fluxes are 17 ± 4, 1.8 ± 0.4, and 36 ± 9 kmol/s, respectively. The flux uncertainties are dominated by (and roughly scale with) the uncertainty of volume transport, here assumed to be ±20%, since we lack sufficient in situ data to fully constrain Anadyr Strait transport. If summertime nutrient depletion depths are 20 m (instead of 10 m assumed previously) this reduces our annually averaged nutrient flux estimates by ∼10%.

3.4. Nutrient Fluxes Through Bering Strait

Mooring data show that Anadyr and Bering Strait property variations are highly covariable due to their strong advective connectivity (Figure 1d). Specifically, at a 17 day lag, low-pass filtered (30-day cutoff period) salinity measurements at N2 and A3 have a correlation coefficient of 0.70 and both records have similar means and dynamic ranges. This modestly tight co-variability implies water is not strongly modified in its transit between the straits, thus we employ the salinity-to-nutrient relationships of Section 3.2 to estimate nutrient fluxes at Bering Strait for past years. For this we use Woodgate (2018) estimates of Bering Strait salinity and transport based on A3 mooring data (See Figure 1a and Section 2.2.2). Although monthly estimates of transport (T_{A3}) and salinity (S_{A3}) begin in 1990, early records are intermittent so we focus on the continuous period of the record, starting in fall 1997.

For September–December and January–April we use the monthly salinity measured at A3 (S_{A3}) and the salinity-nutrient regressions from N2 (i.e., Equation 1) to estimate monthly concentrations for nitrate, phosphate, and silicate at Bering Strait ($NO3_{EST,BS}$, $PO4_{EST,BS}$, and $SiO4_{EST,BS}$, respectively), assuming a vertically unstratified regime. Using T_{A3} and these salinity-estimated nutrient concentrations, Equation 2 provides nutrient flux estimates through Bering Strait ($F_{NO3,BS}$, $F_{PO4,BS}$, $F_{SiO4,BS}$). Since salinity and nutrients are not significantly correlated at N2 from May–August, we do not use salinity parameterization (Equation 1) during these months. Instead, we use in situ observations from the Russian-American Long-Term Census of the Arctic Program (RUSALCA) (Crane & Ostrovskiy, 2015) to estimate the average nutrient concentrations within the strait. From a set of five separate cruises in August spanning 2004–2010, we select stations in close proximity to the strait to estimate the average Bering Strait nutrient cross-section for each year and nutrient parameter (See Figure 1b for nitrate). For all nutrients, there is near-surface nutrient depletion across the whole strait, nutrient-rich subsurface waters from Anadyr Strait in the west, and nutrient-poor waters of the ACC in the east. We compute the mean concentration of each parameter over the entirety of the interpolated cross-sections and find averages of 10.9, 1.3, and 19.2 μmol/kg for nitrate ($NO3_{RUS,BS}$), phosphate ($PO4_{RUS,BS}$), and silicate ($SiO4_{RUS,BS}$), respectively. We use these as representative concentrations for Bering Strait from May–August. While we lack in situ Bering Strait data from

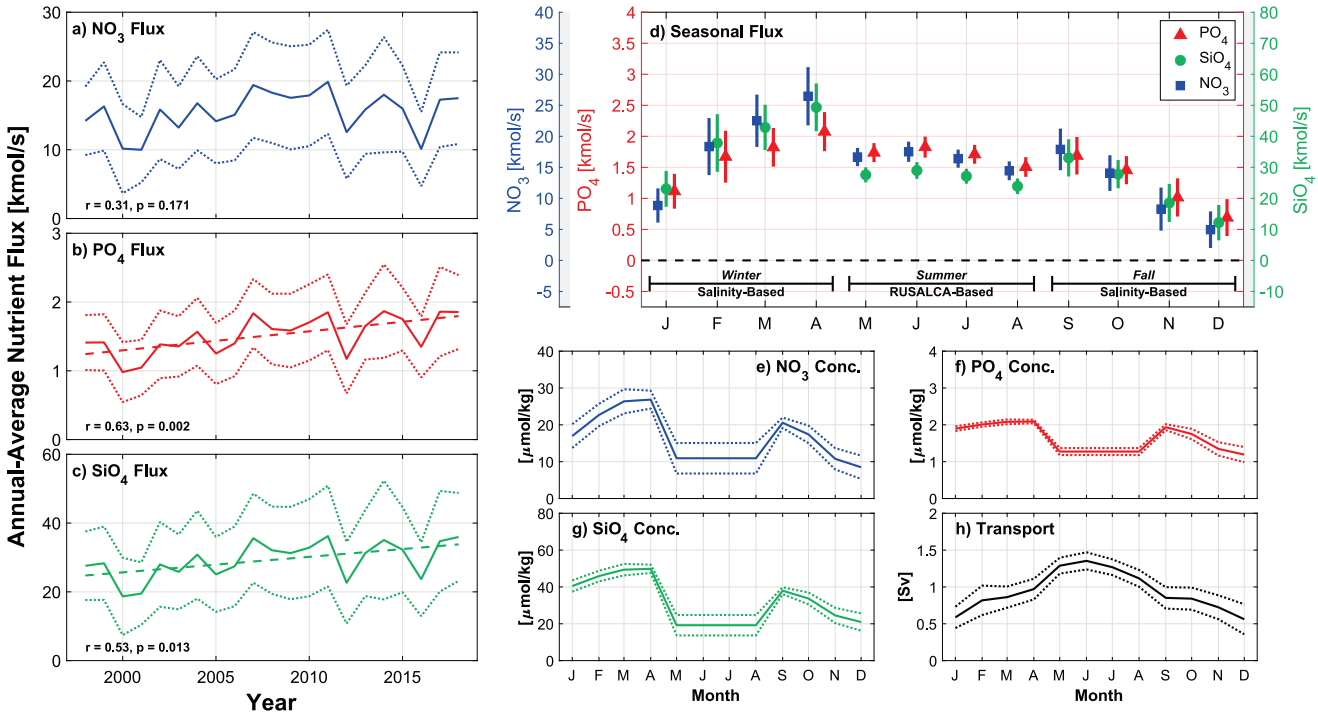

Figure 3. (a–c) Estimated annual average nutrient flux through Bering Strait from 1998 to 2018. Positive values represent poleward flux, dotted lines show the 95% confidence interval (CI), and dashed lines show the linear regression (only shown if significant). (d) The 1997–2018 estimated monthly average nutrient flux through Bering Strait. Symbols are the mean and vertical lines show the 95% CI within each month. (e–h) The monthly averages (solid line) and standard deviation (dashed lines) of nutrient concentrations and transport estimated at Bering Strait.

May–July, SUNA data from N2 suggests this season is typically the least temporally variable (Figure 2f), so averages from August (following most of the growing season's productivity) should provide a serviceable, perhaps conservative representation for the May–August interval. RUSALCA-based concentrations are subsequently coupled with A3 transports to estimate nutrient fluxes from May–August. By combining the RUSALCA-based (May–August) and salinity-based flux estimates (all other months) we construct a continuous monthly record of nutrient flux through Bering Strait from August 1997 to August 2019 (Figure F1 in Supporting Information S1). The period-of-record mean for nitrate, phosphate, and silicate fluxes are 16 ± 6, 1.6 ± 0.5, and 30 ± 11 kmol/s, respectively.

Interannual variability (and uncertainty) is found to be 10–20 (~6), 1.0–1.9 (~0.5), and 18–36 (~11) kmol/s for nitrate, phosphate, and silicate, respectively (Figures 3a–3c). There are statistically significant ($p < 0.05$) long term temporal trends for phosphate ($p < 0.01$) and silicate ($p < 0.02$), but not for nitrate ($p = 0.17$) (See Discussion for possible bias here due to decreasing salinities in the Bering Strait). Sensitivity analysis, where transport (T) and nutrient concentrations (C) are split into mean and anomaly terms ($T = \overline{T} + T'$, $C = \overline{C} + C'$, and nutrient flux is $T{\cdot}C$), shows that increasing transport is responsible for the increase in flux for phosphate and silicate ($|T' \cdot \overline{C}| > |\overline{T} \cdot C'|$), while for nitrate decreased concentrations offset the increased transport ($|T' \cdot \overline{C}| \approx |\overline{T} \cdot C'|$). There is also considerable seasonal variability (Figure 3d, Table T2 in Supporting Information S1). Monthly average fluxes range between about 5 ± 3 to 27 ± 4, 0.7 ± 0.3 to 2.1 ± 0.3, and 12 ± 5 to 50 ± 7 kmol/s for nitrate, phosphate, and silicate respectively, with April maxima and December minima. This timing coincides with months of maximum and minimum salinity, consistent with our salinity-based parameterizations (Equation 1).

4. Discussion

To sustain 50 g C m^{-2} yr^{-1} of new production in the Chukchi Sea, MacDonald et al. (2010) estimate the required Pacific inflow of dissolved inorganic nitrogen is 16.5 kmol/s, close to our estimate of 16 ± 6 kmol/s. Our wintertime nitrate flux estimates at Bering Strait are also consistent with downstream estimates at Icy Cape by Mordy

et al. (2020), assuming ∼40% of Bering Strait transport (Stabeno et al., 2018) reaches their central Chukchi mooring array (e.g., 6 ± 2 kmol/s compared to 18 ± 5 kmol/s found here during February). However, our Bering Strait nutrient fluxes are significantly higher (∼25%–75%) than those estimated by Torres-Valdes et al. (2013). The majority of the discrepancy is rooted in methodological differences, with our single year, but year-round time series observations allowing a seasonally-resolved approach. Torres-Valdes et al. (2013) use temporally static nutrient concentrations based on one summer transect along with seasonally changing transport estimates. Torres-Valdes et al. (2013) used a Bering Strait average nitrate concentration of 10 μmol/kg (August 2005), whereas our annually averaged (for 1998–2018) concentration is ∼16 μmol/kg, which is roughly the same fractional difference between their nitrate flux estimate and that found here.

Recently, Zhou et al. (2021) used a three-dimensional ocean-sea ice-biogeochemical model to simulate nitrate flux through Bering Strait from 1998 to 2015 and found values of ∼12 kmol/s during February–May, and ∼8 kmol/s much of the remainder of the year. While that seasonality has loose qualitative agreement with the monthly variability found here (Figure 3d), their annual average of 9.63 kmol/s is lower than our 16 ± 6 kmol/s, and we find greater seasonality (∼5–25 kmol/s vs. ∼8–12 kmol/s). A possible explanation for the discrepancy of the annual averages is that Zhou et al. (2021) found simulated nitrate concentrations upstream of Anadyr Strait that were significantly lower (by ∼5 μmol/kg) than in situ concentrations, which may translate to lower Bering Strait nitrate fluxes.

We know of no long-term trends of deep water thermohaline and nutrient composition in the Bering Sea basin, though the stability of the salinity-nutrient relationships over the multi-decadal period of record (1998–2018) is a critical assumption for our methodology, given these relationships are only estimated from the one yearlong N2 mooring deployment (2017–2018). The January–April salinity-nutrient measurements from N2 are near the mixing line between deep nutrient-rich and shallow nutrient-poor waters established from hydrographic data (Figure 2a) collected up to 13 years before the N2 deployment, possibly suggesting long-term stability. However, Woodgate (2018) observes a multi-decadal freshening trend at Bering Strait, possibly due to glacier ablation in the Gulf of Alaska. Our salinity-nutrient relationships are based on mixing between high-salinity high-nutrient Pacific Basin waters and low-nutrient low-salinity shelf water, so changes over time to the shallow, low-salinity end member could impact our estimates. If Bering Shelf water has become fresher (with constant nutrient content), we may slightly overestimate nutrient concentrations with our parameterizations (though we lack data to examine this).

Prominent discontinuities between estimated fluxes on either side of the summer season (Figure 3d) mark the changeover between salinity-based nutrient estimates and RUSALCA measurements used for May–August, and demonstrate likely methodological limitations. There are different uncertainties associated with each of the methods, but discontinuities may also partially reflect the seasonally varying nutrient uptake cycle. Brown et al. (2011) estimate that 54% of the regional annual net primary production occurs from May to July, so phytoplankton blooms during this interval draw down nutrient concentrations, thereby reducing Arctic-bound nutrient fluxes. The northern Bering and southern Chukchi Seas are known for high (250–300 g C m^{-2} yr^{-1}) phytoplankton productivity (Grebmeier et al., 1988; Sambrotto et al., 1984; Springer, 1988; Walsh et al., 1989). Though nutrient consumption during transit between Anadyr and Bering Strait is unknown, we can crudely estimate this by assuming half the total production (∼150 g C m^{-2}) occurs evenly over the ∼50 m deep shelf from May–July. The expected drawdown during the 2-week advective period from Anaydr to Bering Strait would be ∼6 μmol N kg^{-1} (assuming a Redfield ratio of 16N:106C), and the remainder of the year is ∼2 μmol N kg^{-1}. Since our flux estimates only use Anadyr salinity-nutrient relations from September–April, and nutrient concentrations during May–August are based on late-summer RUSALCA observations directly at Bering Strait, we expect only modest error (∼3 μmol N kg^{-1}) from biotic drawdown in Chirikov Basin.

The estimated nitrate, phosphate, and silicate flux in Anadyr Strait for the N2 mooring deployment period over September 2017 – April 2018 was 17 ± 4, 1.8 ± 0.2, and 37 ± 5 kmol/s, respectively (Section 3.3). During the same interval at Bering Strait, fluxes are estimated to be higher, at 24 ± 8, 2.5 ± 0.8, and 52 ± 16 kmol/s. Volume transport through Anadyr Strait is weaker than that through Bering Strait (∼80%; Danielson et al., 2014), but the nutrient delivery through Bering Strait is largely of Anadyr origin (e.g., Figure 1), so the difference in nutrient flux is unlikely explained by volume transport alone. Though the uncertainty ranges of the Anadyr and Bering Strait fluxes overlap, it is possible the larger mean values at Bering Strait are partially due to the southern branch of the Anadyr Current, which on average flows eastward along the south shore of St. Lawrence Island (Danielson

et al., 2006). Thus, our Anadyr Strait estimates could underestimate the total nutrient flux carried poleward from the Gulf of Anadyr. However, we presently lack data to quantify this component or other sources and losses, such as benthic remineralization and denitrification.

Estimates of volume transport through Bering Strait used here (Section 3.4, Woodgate, 2018) do not correct for ACC influences, an additional source of uncertainty. However, the fractional correction for volume transport is ~10% (Woodgate, 2018), and ACC water is known for being nutrient deplete (Danielson et al., 2017), so it is unlikely the ACC contributes a significant fraction of the overall nutrient supply to the Arctic. These fluxes also do not include other forms of nitrogen (e.g., ammonium, particulate organic nitrogen), that may be important for primary producers. While ammonium concentrations are higher on the Bering Shelf (Mordy et al., 2008, 2010), they may be less important for slope-derived water, such as the Anadyr Current.

Woodgate (2018) described a multi-year trend of increasing transport and declining salinity. For our parameterizations this introduces competing effects, as increased volume transport favors increased nutrient flux, while decreasing salinity translates to lower assumed nutrient concentration and fluxes (Equations 1 and 2). Using salinity-nutrient parameterizations established at N2, we find silicate and phosphate fluxes have likely increased significantly from 1998 to 2018, while nitrate has a weak, insignificant positive trend ($p = 0.17$). Though nitrate, phosphate, and silicate are all well correlated with salinity during non-summer months ($r \geq 0.89$), changes in salinity correspond to a larger fractional change in $NO3_{EST,BS}$ than either $PO4_{EST,BS}$ or $SiO4_{EST,BS}$ (Fig. 2 b–d). Thus, long term decreases in salinity at Bering Strait drive a decrease in computed nitrate, which when combined with the increase in volume flux means $F_{NO3,BS}$ remains relatively steady. Salinity variability causes less fractional change in $PO4_{EST,BS}$ and $SO4_{EST,BS}$, such that the increased transport is the determining factor in long term changes of $F_{PO4,BS}$ and $F_{SiO4,BS}$ (Section 3.4).

5. Conclusions

Though we calculate significant decadal trends for phosphate and silicate, but not for nitrate, we caution that these results are built upon the assumption that salinity-nutrient reletionships are static across years. Verifying this is vital for validating our trend conclusions. Independent of potential decadal trends, we also find that nutrient flux through Bering Strait is considerably higher than previous estimates. Torres-Valdes et al. (2013) found that Bering Strait is a substantial source of annual nutrient supply to the broader Arctic Ocean (21 ± 4%, 35 ± 6%, and 61 ± 11% for nitrate, phosphate, and silicate, respectively). Our analysis suggests Bering Strait may be a proportionally more significant source of Arctic nutrients than previously appreciated.

Acknowledgments
The authors thank the captain and crew of R/V Sikuliaq and UAF mooring technician Pete Shipton for successful cruises. This work was funded by Arctic Integrated Ecosystem Research Program grants A91-99a, A91-00a to the Arctic Shelf Growth, Advection, Respiration and Deposition rate experiments project. CWM was funded by Arctic IERP grant A92. The Arctic IERP was supported by the North Pacific Research Board, the Collaborative Alaskan Arctic Studies Program (formerly the North Slope Borough/Shell Baseline Studies Program), the Bureau of Ocean Energy Management, and the Office of Naval Research Marine Mammals and Biology Program. This publication is partially funded by the Cooperative Institute for Climate, Ocean, & Ecosystem Studies (CIOCES) under NOAA Cooperative Agreement NA20OAR4320271. This is NPRB publication #ArcticIERP-46, PMEL publication #5350, EcoFOCI publication #1024, and CICOES publication #2022-1177. Bering Strait moorings are funded by NSF-AON (PLR-1304052, PLR-1758565).

Data Availability Statement

CTD-corrected Aqua Monitor data can be found in Table T3 of Supporting Information S1. Raw and CTD-corrected Aqua Monitor nutrient data can also be found at https://doi.org/10.24431/rw1k6cn. N2 SUNA nitrate data and shipboard casts for calibrations are at https://doi.org/10.24431/rw1k6cp. Russian-American Long-Term Census of the Arctic Program nutrients are at https://doi.org/10.24431/rw1k6ci. N2 ADCP date are at https://doi.org/10.24431/rw1k59y, and N2 CTD data are at https://doi.org/10.24431/rw1k5bf. Mooring data from A3 (2017–2018) are located at https://doi.org/10.18739/A2PZ51M3V. Bering Strait transport and salinity are available at http://psc.apl.washington.edu/BeringStrait.html and https://doi.org/10.18739/A2PZ51M3V.

References

Becker, S., Aoyama, M., Woodward, E. M. S., Bakker, K., Coverly, S., Mahaffey, C., & Tanhua, T. (2020). GO-SHIP repeat hydrography nutrient manual: The precise and accurate determination of dissolved inorganic nutrients in seawater, using continuous flow analysis methods. *Frontiers in Marine Science*, *7*, 908. https://doi.org/10.3389/fmars.2020.581790

Brown, Z. W., Dijken, G. L. V., & Arrigo, K. R. (2011). A reassessment of primary production and environmental change in the Bering Sea. *Journal of Geophysical Research*, *116*, C08014. https://doi.org/10.1029/2010JC006766

Coachman, L. K. (1993). On the flow field in the Chirikov Basin. *Continental Shelf Research*, *13*(5–6), 481–508. https://doi.org/10.1016/0278-4343(93)90092-C

Crane, K., & Ostrovskiy, A. (2015). Introduction to the special issue: Russian-American long-term census of the Arctic (RUSALCA). *Oceanography*, *28*(3), 18–23. https://doi.org/10.5670/oceanog.2015.54

Daniel, A., Laës-Huon, A., Barus, C., Beaton, A. D., Blandfort, D., Guigues, N., et al. (2020). Toward a harmonization for using in situ nutrient sensors in the marine environment. *Frontiers in Marine Science*, *6*. https://doi.org/10.3389/fmars.2019.00773

Danielson, S., Aagaard, K., Weingartner, T., Martin, S., Winsor, P., Gawarkiewicz, G., & Quadfasel, D. (2006). The St. Lawrence polynya and the Bering shelf circulation: New observations and a model comparison. *Journal of Geophysical Research*, *111*, C09023. https://doi.org/10.1029/2005JC003268

Danielson, S., Curchitser, E., Hedstrom, K., Weingartner, T., & Stabeno, P. (2011). On ocean and sea ice modes of variability in the Bering Sea. *Journal of Geophysical Research*, *116*, C12034. https://doi.org/10.1029/2011JC007389

Danielson, S. L., Eisner, L., Ladd, C., Mordy, C., Sousa, L., & Weingartner, T. J. (2017). A comparison between late summer 2012 and 2013 water masses, macronutrients, and phytoplankton standing crops in the northern Bering and Chukchi Seas. *Deep-Sea Research Part II Topical Studies in Oceanography*, *135*, 7–26. https://doi.org/10.1016/j.dsr2.2016.05.024

Danielson, S. L., Weingartner, T. J., Hedstrom, K. S., Aagaard, K., Woodgate, R., Curchitser, E., & Stabeno, P. J. (2014). Coupled wind-forced controls of the Bering-Chukchi shelf circulation and the Bering Strait throughflow: Ekman transport, continental shelf waves, and variations of the Pacific-Arctic sea surface height gradient. *Progress in Oceanography*, *125*, 40–61. https://doi.org/10.1016/j.pocean.2014.04.006

Grebmeier, J., Bluhm, B. A., Cooper, L. W., Danielson, S. L., Arrigo, K. R., Blanchard, A. L., et al. (2015). Ecosystem characteristics and processes facilitating persistent macrobenthic biomass hotspots and associated benthivory in the Pacific Arctic. *Progress in Oceanography*, *136*, 92–114. https://doi.org/10.1016/j.pocean.2015.05.006

Grebmeier, J., McRoy, C., & Feder, H. (1988). Pelagic-benthic coupling on the shelf of the northern Bering and Chukchi Seas. I. Food supply source and benthic bio-mass. *Marine Ecology Progress Series*, *48*, 57–67. https://doi.org/10.3354/meps048057

Huntington, H. P., Danielson, S. L., Wiese, F. K., Baker, M., Boveng, P., Citta, J. J., et al. (2020). Evidence suggests potential transformation of the Pacific Arctic ecosystem is underway. *Nature Climate Change*, *10*(4), 342–348. https://doi.org/10.1038/s41558-020-0695-2

Lewis, K. M., & Arrigo, K. R. (2020). Ocean color algorithms for estimating chlorophyll a, CDOM absorption, and particle backscattering in the ArcticOcean. *Journal of Geophysical Research: Oceans*, *125*, e2019JC015706. https://doi.org/10.1029/2019JC015706

MacDonald, R. W., Anderson, L. G., Christensen, J. P., Miller, L. A., Semiletov, I. P., & Stein, R. (2010). The Arctic Ocean. In K.-K. Liu, L. Atkinson, R. Qui~nones, & L. Talaue- McManus (Eds.), *Carbon and nutrient fluxes in continental margins: A global synthesis* (pp. 291–303). Springer Berlin Heidelberg.

Mordy, C. W., Bell, S., Cokelet, E. D., Ladd, C., Lebon, G., Stabeno, P., et al. (2020). Seasonal and interannual variability of nitrate in the eastern Chukchi Sea: Transport and winter replenishment. *Deep-Sea Research Part II Topical Studies in Oceanography*, *177*, 104807. https://doi.org/10.1016/j.dsr2.2020.104807

Mordy, C. W., Eisner, L. B., Proctor, P., Stabeno, P., Devol, A. H., Shull, D. H., et al. (2010). Temporary uncoupling of the marine nitrogen cycle: Accumulation of nitrite on the Bering Sea shelf. *Marine Chemistry*, *121*(1–4), 157–166. https://doi.org/10.1016/j.marchem.2010.04.004

Mordy, C. W., Stabeno, P. J., Righi, D., & Menzia, F. A. (2008). Origins of the subsurface ammonium maximum in the southeast Bering Sea. *Deep Sea Research Part II: Topical Studies in Oceanography*, *55*(16–17), 1738–1744. https://doi.org/10.1016/j.dsr2.2008.03.005

Polyakov, I. V., Rippeth, T. P., Fer, I., Alkire, M. B., Baumann, T. M., Carmack, E. C., et al. (2020). Weakening of cold halocline layer exposes sea ice to oceanic heat in the eastern Arctic Ocean. *Journal of Climate*, *33*(18), 8107–8123. https://doi.org/10.1175/JCLI-D-19-0976.1

Sambrotto, R. N., Goering, J. J., & McRoy, C. P. (1984). Large yearly production of phytoplankton in the western Bering Strait. *Science*, *225*(4667), 1147–1150. https://doi.org/10.1126/science.225.4667.1147

Springer, A. M. (1988). *The paradox of pelagic food webs on the Bering–Chukchi continental shelf* (Dissertation). University of Alaska Fairbanks.

Stabeno, P., Kachel, N., Ladd, C., & Woodgate, R. (2018). Flow Patterns in the Eastern Chukchi Sea: 2010–2015. *Journal of Geophysical Research: Oceans*, *123*(2), 1177–1195. https://doi.org/10.1002/2017JC013135

Torres-Valdés, S., Tsubouchi, T., Bacon, S., Naveira-Garabato, A. C., Sanders, R., McLaughlin, F. A., et al. (2013). Export of nutrients from the Arctic Ocean. *Journal of Geophysical Research: Oceans*, *118*, 1625–1644. https://doi.org/10.1002/jgrc.20063

Walsh, J. J., McRoy, C. P., Coachman, L. K., Goering, J. J., Nihoul, J. J., Whitledge, T. E., et al. (1989). Carbon and nitrogen cycling within the Bering/Chukchi Seas: Source regions for organic matter effecting AOU demands of the Arctic Ocean. *Progress in Oceanography*, *22*(4), 277–359. https://doi.org/10.1016/0079-6611(89)90006-2

Wang, M., Yang, Q., Overland, J. E., & Stabeno, P. (2018). Sea-ice cover timing in the Pacific Arctic: The present and projections to mid-century by selected CMIP5 models. *Deep-Sea Research II*, *152*, 22–34. https://doi.org/10.1016/j.dsr2.2017.11.017

Woodgate, R. A. (2018). Increases in the Pacific inflow to the Arctic from 1990 to 2015, and insights into seasonal trends and driving mechanisms from year-round Bering Strait mooring data. *Progress in Oceanography*, *160*, 124–154. https://doi.org/10.1016/j.pocean.2017.12.007

Woodgate, R. A., Stafford, K. M., & Prahl, F. G. (2015). A synthesis of year-round interdisciplinary mooring measurements in the Bering Strait (1990–2014) and the RUSALCA years (2004–2011). *Oceanography*, *28*(3), 46–67. https://doi.org/10.5670/oceanog.2015.57

Zhou, J., Luo, X., Xiao, J., Wei, H., Zhao, W., & Zheng, Z. (2021). Modeling the seasonal and interannual variations in nitrate flux through Bering Strait. *Journal of Marine Systems*, *218*, 103527. https://doi.org/10.1016/j.jmarsys.2021.103527